

Neutral competition boosts chaos in food webs

Pablo Rodríguez-Sánchez ^{*1}, Egbert H. van Nes ^{†1}, and Marten
Scheffer ^{‡1}

¹Department of Aquatic Ecology, Wageningen University, The
Netherlands

August 2, 2018

Manuscript type: article.

Keywords: coexistence, competition, neutral competition, biodiversity para-
dox.

Manuscript elements: 5 figures, 1 table, 1 online appendix (including 8 fig-
ures and 2 tables).

The authors wish to be identified to the reviewers.

*pablo.rodriguezsanchez@wur.nl

†egbert.vannes@wur.nl

‡marten.scheffer@wur.nl

Abstract

14 Near-neutrality of competition has been proposed to facilitate coexis-
tence of species because it slows down competitive exclusion, thus mak-
16 ing it easier for equalizing mechanisms to maintain diverse communities.
An unrelated line of work has shown that chaos can promote coexis-
18 tence of many species in super-saturated communities. By analyzing a
set of numerically simulated food webs, here we link those previously
20 unrelated findings. We show that near-neutrality of competition at the
prey's trophic level, in the presence of interactions with natural enemies,
increases the chances of developing chaotic dynamics. Our results sug- 22
gest that near-neutrality may promote biodiversity in two ways: through
reducing the rates of competitive displacement and through promoting 24
non-equilibrium dynamics.

1 Background

26

Ever since Darwin, the idea that species must be sufficiently different to be able to coexist is deeply rooted in the history of biological thinking. Indeed, the principle of competitive exclusion is intuitively straightforward, and elegant mathematical underpinning [1] helped making it one of the cornerstones of ecological theory. Nevertheless, on a closer examination, natural communities often seem to harbor far more species that may be reasonably explained from niche separation. Plankton communities, where many species coexist with little room for differentiation, have served as an early example [2, 3], inspiring the legendary ecologist G. Evelyn Hutchinson to ask the simple but fundamental question "*why are there so many kinds of animals?*" [3]. Since then many mechanisms have been shown to help similar species coexist. As Hutchinson already proposed himself, fluctuations in conditions may prevent reaching equilibrium at which species would be outcompeted. Also, natural enemies including pests and parasites tend to attack the abundant species more than rare species, and such a "*kill the winner*" [4] mechanism promotes diversity by preventing one species to take all the resources and outcompete the rest.

28

30

32

34

36

38

40

42

In the extensive literature on mechanisms that can prevent competitive exclusion there are two newcomers that radically differ from the rest and have created quite a stir: neutrality and chaos. The neutral theory of biodiversity introduced by Hubbell [5] proposes that species that are entirely equivalent can coexist in a neutral way because none is able to outcompete the other. The concept of completely equivalent species has met skepticism as it is incompatible with the idea that all species are different. However, it turns out that also "*near-neutrality*" arises robustly in models of competition and evolution and may boost the chances for coexistence [6–9]. Support for such near-neutrality has been found in a wide range of communities [6, 10–13]. The second relatively new and controversial mechanism that may prevent competitive exclusion is "*super-saturated coexistence*" in communities that display chaotic dynamics [14].

44

46

48

50

52

54

This is in a sense analogous to the prevention of competitive exclusion in fluctuating environments, except that deterministic chaos may arise in autonomous non-linear systems without any external perturbation. Although there has been much debate about the question whether such internally driven complex dynamics plays an important role in ecosystems, several studies support the idea that chaos can be an essential ingredient of natural dynamics [15]

Surprisingly, while the potential roles of chaos and neutrality have been intensely debated, studies seem to have explored how these two fundamental drivers of diversity could be causally related. Here we address this question using simple food-web models. We vary the level of neutrality in the competition between prey species and analyze its effect on the likelihood of generating chaotic dynamics.

2 Methods

2.1 Model description

We focused our attention on food webs with two trophic levels, one of consumers and another of prey (see figure in the Online Appendix). The consumers predate on the prey, and the prey populations compete among each other for a common source of resources.

The dynamics were modelled as a system of ordinary differential equations. We used the Rosenzweig-MacArthur predator-prey model [16] generalized to a higher number of species (see [17] and Online Appendix).

Our model contains n_P prey species and n_C predator species. The prey's populations grow logistically under the influence of intra and interspecific competition. The intensities of both these competitions are coded in the matrix A . The coupling of both groups happens via predation. Obviously, predation has a negative effect for prey and a positive one for predators. The relative preference that predators show to each prey is coded in the matrix S . In the absence

of prey, the predators' populations just decay exponentially. Prey immigration
 from neighboring areas has been added to the classical model in order to avoid
 unrealistic long-stretched cycles with near extinctions [17].

In mathematical notation, the system reads:

$$\begin{cases} P'_i(t) = r_i(P)P_i - P_i \sum_{j=1}^{n_C} g_j(P)S_{ji}C_j + f & : i = 1..n_P \\ C'_j(t) = -lC_j + eg_j(P)C_j \sum_{i=1}^{n_P} S_{ji}P_i & : j = 1..n_C \end{cases} \quad (1)$$

where $P_i(t)$ represents the biomass of prey species i at time t and $C_j(t)$
 the biomass of predator species j at time t . The auxiliary functions $r_i(P)$ and
 $g_j(P)$ have been respectively chosen to generalize the logistic growth and the
 Holling type II saturation functional response [18] to a multispecies system when
 inserted into equation 1. They are defined as:

$$r_i(P) = r \left(1 - \frac{1}{K} \sum_{k=1}^{n_P} A_{ik}P_k \right) \quad (2)$$

$$g_j(P) = \frac{g}{\sum_{i=1}^{n_P} S_{ji}P_i + H} \quad (3)$$

For details about the parameters used, please refer to subsection 2.2. For a
 detailed derivation of equation 1, see Online Appendix.

2.2 Parameterization

We parameterized our model as a freshwater plankton system based on Dakos'
 model [19]. Dakos' model uses a Rosenzweig-McArthur multi-species model
 with two trophic levels, and parameterizes it to describe a zooplankton - phyto-
 plankton system. Unlike Dakos, who uses seasonally changing parameters, our
 parameters were assumed to be independent of time (see table 1).

Symbol	Interpretation	Value	Units
r	Maximum growth rate	0.50	d^{-1}
K	Carrying capacity	10.00	$mg\ l^{-1}$
g	Predation rate	0.40	d^{-1}
f	Immigration rate	10^{-5}	$mg\ l^{-1}\ d^{-1}$
e	Assimilation efficiency	0.60	1
H	Half-saturation constant	2.00	$mg\ l^{-1}$
l	Predator's loss rate	0.15	d^{-1}
S	$n_C \times n_P$ predator preference matrix	$S_{ij} \in (0, 1)$	1
A	$n_P \times n_P$ competition matrix	See section 2.2.1	1

Table 1: Values and meanings of the parameters used in our numerical experiment. The elements of the predation matrix S are drawn from a uniform probability distribution, bounded between 0 and 1.

2.2.1 Competition matrix

Our main purpose is to analyze the effect of different degrees of heterogeneity in the competition matrix on the long term dynamics exhibited. In order to simulate and quantify this heterogeneity, we introduce the competition parameter ϵ . This dimensionless parameter was used to build a competition matrix A , whose diagonal terms are identically 1, and whose non-diagonal terms are drawn from a uniform probability distribution centered at $1 + \epsilon$ and with a given width (here we chose $w = 0.2$).

106

Defined this way, the parameter ϵ allows us to travel continuously from strong intraspecific ($\epsilon < 0$) to strong interspecific competition ($\epsilon > 0$), meeting neutral competition near $\epsilon = 0$ (see figure 1).

108

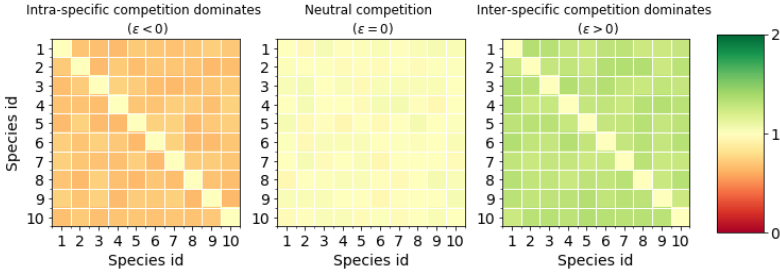


Figure 1: The competition matrix on the left is a clear case of dominant intraspecific competition. The central one represents a case of neutral competition. The matrix in the right panel shows a case of dominant interspecific competition. The difference between them is the relative size of the non-diagonal elements respective of the diagonal ones. This qualitative property of the competition matrices is controlled by the competition parameter ϵ .

2.3 Numerical experiment

110

Depending on the parameters and initial conditions, a system like the one described in equation 1 can give rise to three types of qualitative behaviour. Each of them roughly corresponds to a different type of attractor (see figure 2). The first one, a stable point attractor, generates a constant species composition. Secondly, limit cycle (and limit tori) attractors give rise to periodically (or quasiperiodically) changing species composition. Lastly, we'll refer as chaotic to attractors that, while remaining bounded, do not fit in any of the previous categories.

112

114

116

118

Our target is to estimate the probability of reaching one of such chaotic attractors under different assumptions about competition. In order to achieve this, we swept among 23 different values of the competition parameter ϵ (defined in section 2.2.1). We simulated a set of 200 ecosystems per competition parameter value. This amounts to a total of 4600 simulated ecosystems. These ecosystems differ from each other in initial conditions, predation rates S_{ji} , and competition

120

122

124

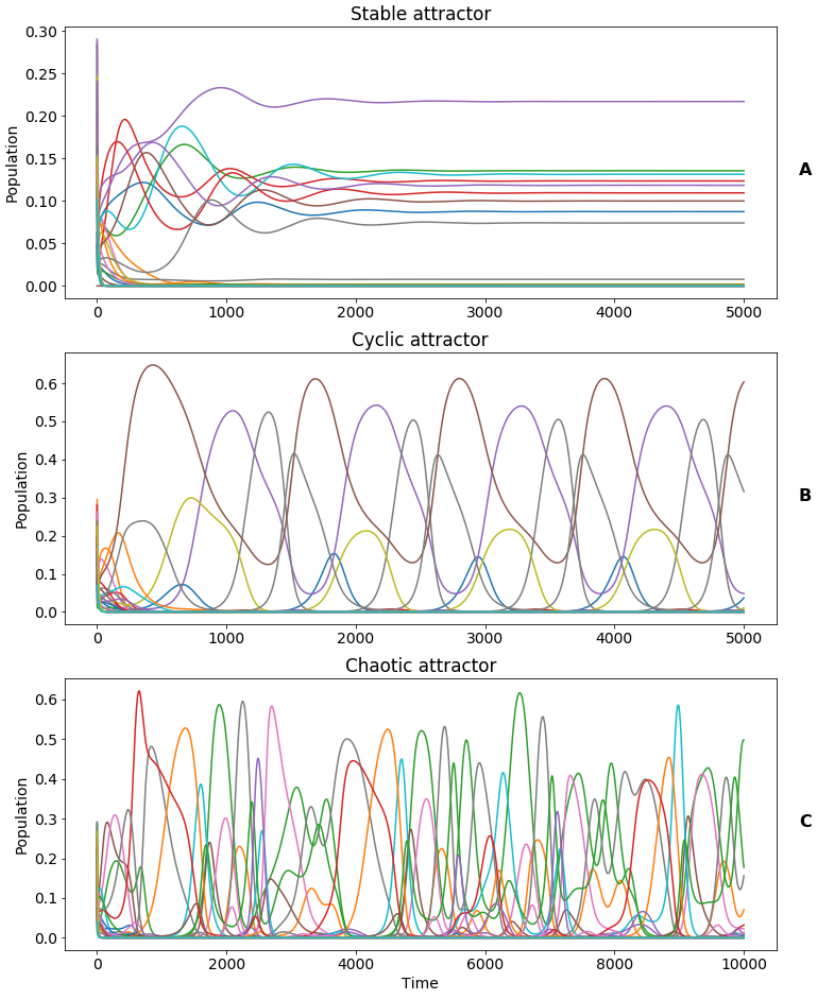


Figure 2: Our family of models generates time series of the population of each species. The time series can be classified in 3 qualitative types depending on their asymptotic behaviour: *stable*, *periodic* and *chaotic*. In **panel A**, the system reaches a stable attractor after a transient time. In **panel B**, a periodic attractor, with an approximate period of 1000 days, is reached after the transient time. The system in **panel C** never reaches a stable nor a cyclic attractor, but a chaotic one.

matrices, all of them sampled from probability distributions (see 2.2). Ecosystems grouped by competition parameter ϵ , despite not being identical, exhibit the same competition type (see 2.2.1).

Numerical methods were used to integrate each realization of the equation 1. A first stabilizing run of 2000 days is executed in order to get closer to the attractor. Simulating for 5000 more days, we obtain trajectories in the vicinity of the attractor.

We considered chaotic those time series that triggered the Gottwald - Melbourne test (see [20] and Online Appendix). Using this approach, we classified each individual simulation as *chaotic* or *non-chaotic*.

The ratio of attractors found to be chaotic can be used to estimate the probability of a family of ecosystems to develop chaotic behaviour. Grouping those ecosystems by competition parameter ϵ , we explored the relationship between the probability of chaos and the degree of heterogeneity.

Additionally, the experiment was repeated for food webs of different sizes. In our simulations, we kept a ratio of 2:3 for the number of species at the consumer and the prey level.

In the spirit of reproducible research, we made available the scripts used to obtain our conclusions and generate our figures [21].

3 Results

Plotting the probability of chaos against the competition parameter (see figure 3), we observe a clear maximum around $\epsilon = 0$. The likelihood of chaotic behaviour for neutral competition at the prey's trophic level is thus higher than for dominant inter or intraspecific competition. This result remains true for systems with a different number of species (figures 3 and 4).

The overall likelihood of chaos, which can be interpreted as the area under the curve in figure 3, increases with the size of the food web. This effect should not be surprising: the more dimensions the phase space has, the easier is to

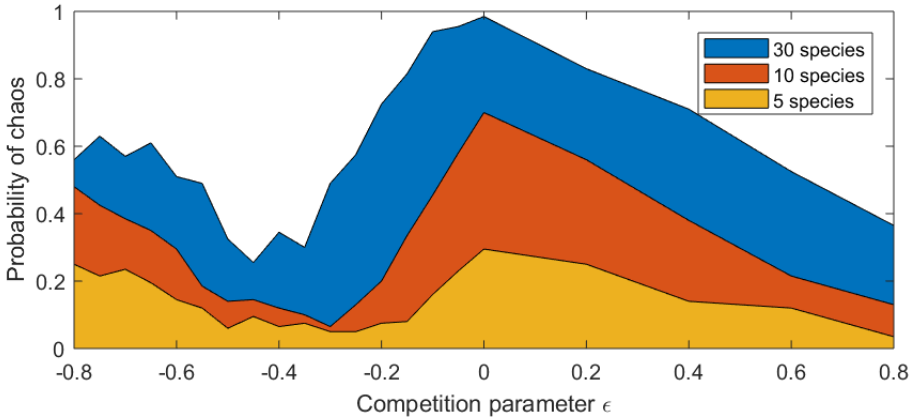


Figure 3: Results for a low, medium and high dimensional system. The consumers’ population is fixed as $2/3$ of the prey’s population. Notice how the probability of chaos has a local maximum around $\epsilon = 0$. The effect remains true for systems with different number of species. The overall probability of chaos, understood as the area under the curve, grows with the system size.

fulfill the requirements of the complex geometry of a chaotic attractor [22].

Even in those higher dimensional cases, there is still a clear maximum at neutral competition.

Another local maximum was observed for low values of ϵ . This means that weak competitive coupling also promotes chaos in our model.

Between both local maxima there is obviously a local minimum whose exact position differed between simulations.

4 Discussion

The asymptotic dynamics of our model are affected by the strength of intraspecific competition compared to interspecific competition. Interestingly, we find that competition closer to neutrality significantly increases the chances of chaotic behaviour. This suggests that in a system with predation, near-neutrality at the competition level may increase the probability of complex

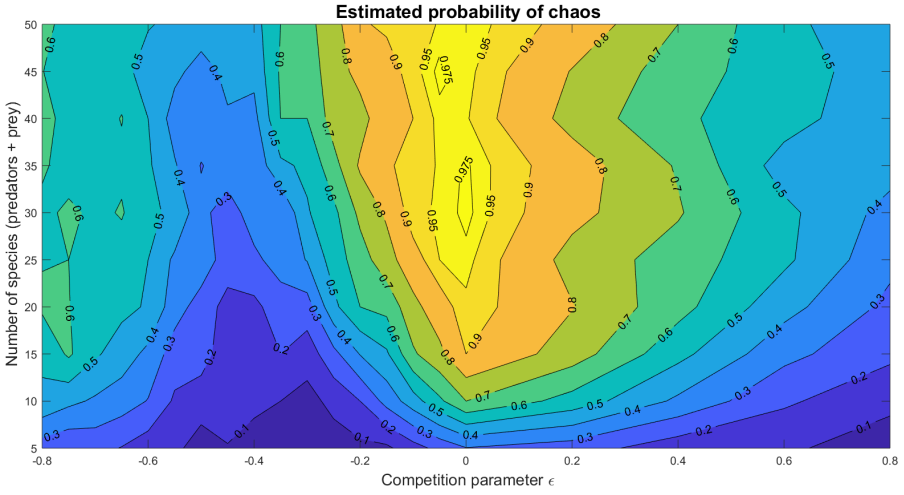


Figure 4: Contour map showing the probability of chaos for various competition parameters (horizontal axis) and number of species (vertical axis). The consumers' population is fixed as $2/3$ of the prey's population. Notice that chaotic attractors appear more easily (i.e., for smaller systems) the closer is the competition to neutral (i.e., $\epsilon = 0$).

166 dynamics if the species are not equally prone to predation. Provided that the
 competitive exclusion principle rests on the assumption of equilibrium, near-
 168 neutrality reduces the chances of the principle to be applicable, improving the
 chance for a higher number of coexisting species if dynamics are chaotic [14].
 170 Additionally, this observation suggests that the hypothesis of non-equilibrium
 and Hubbell’s hypothesis of neutrality are not completely independent (see fig-
 172 ure 5). Our model shows another local maximum for the probability of chaos for
 weak competition coupling. We consider this a reasonable result, as predation
 174 is known to be the main driver of chaos in this kind of models [17].

In the spirit of mathematical modelling, we chose the simplest realization
 176 required for the effects to be observed. We didn’t use Allee effect, nor noise,
 and the functional form of each term has been chosen to account for satiation
 178 and saturation in the simplest possible ways. The choice of a two-level model
 may seem in contradiction with the pursue of simplicity, but actually it is a
 180 fundamental requirement for the effect under research to take place. In the
 absence of a predator level, chaos will never develop in a model with neutral
 182 competition. The reason for this is that if all interactions become equally strong,
 the differences among species at the same trophic level fade out. This makes
 184 labeling each species meaningless, and thus the prey-only system can be reduced
 to a single differential equation, that of the total prey population (see Online
 186 Appendix for details). A classical corollary of the Poincaré-Bendixson theorem is
 that autonomous systems with less than 3 dimensions cannot exhibit chaos [22].

188 For simplicity, both the competition and predation parameters were drawn
 from probability distributions. The interactions in our system can be interpreted
 190 as a weighted network with a high connectivity. In nature, trophic networks tend
 to show modular structure with various clusters [23]. Our simplified model could
 be interpreted as representing one of those densely connected modules.

192

It is known that the asymptotic behaviour of this kind of systems can be
 very sensitive to the parameters choice. In particular, introducing correlations

194

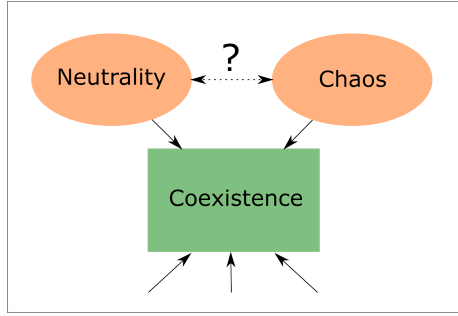


Figure 5: In our model, neutrality and chaos are not independent explanations of coexistence.

between parameters can greatly modify the probabilities of chaotic attractors to be reached (see for instance [24], in response to the letter [25]). In the present paper we didn't introduce any correlation, i.e., all our random parameters were drawn independently from the others. Studying the effect of different physiological scenarios (in the sense of [24], that is, constrains between the parameters) on the probabilities of chaos could be a continuation to this paper.

Due to the large number of simulations made, we had to rely on automatic methods for detecting chaos. Automatic detection of chaos by numerical methods has fundamental limitations, especially for high dimensional systems like ours. Most of them can be boiled down to the fact that, in general, numerical methods cannot distinguish robustly between long, complicated transients and genuine chaos. We think that our approach to chaos detection, despite being open to improvement, suffices to detect the overall patterns (see Online Appendix for a more detailed discussion).

Our results suggest a fundamentally new way in which near-neutrality may promote biodiversity. In addition to weakening the forces of competitive exclusion [7], our analyses reveal that near neutrality may boost the chances for chaotic dynamics. As chaos in turn may facilitate super-saturated co-existence, our findings point to a potentially widespread mechanism of maintaining biodiversity.

5 Acknowledgments

216 The preliminary analysis of this model was performed using GRIND for Mat-
lab (<http://www.sparcs-center.org/grind>). Additionally, we thank Tobias
218 Oertel-Jäger, Sebastian Wieczorek, Peter Ashwin, Jeroen Lamb, Martin Ras-
mussen, Cristina Sargent, Jelle Lever, Moussa N'Dour, Iñaki Úcar, César Ro-
220 dríguez and Sebastian Bathiany for their useful comments and suggestions.

This work was supported by funding from the European Union's *Horizon*
222 *2020* research and innovation programme for the *ITN CRITICS* under Grant
Agreement Number 643073.

224 A Online appendix

This is the Online Appendix for the paper:

226 Rodríguez-Sánchez P, van Nes EH, Scheffer M. *Neutral competition boosts
chaos in food webs.*

228 A.1 Generalized multispecies predation models

A.1.1 General properties of predation models

Most predation models based on differential equations follow a structure like 230
this:

$$\begin{cases} P'(t) = Growth(P) - Predation(P, C) \\ C'(t) = -Loss(C) + GrossGrowth(P, C) \end{cases} \quad (4)$$

where P represents the biomass of the prey population, and C the biomass 232
of the consumer/predator population. The functional dependencies have been
explicitly written in order to remark the fact that the coupling of the system 234
happens via the *Predation* and *GrossGrowth* terms.

It is important to note that, in models like this, all deaths at the prey's level 236
are due to predation. All deaths caused by predation are invested in consumer's
growth. Therefore the following relation must be true: 238

$$GrossGrowth(P, C) = e \cdot Predation(P, C) \quad (5)$$

where e represents the efficiency of the energy transfer process. Equation 5,
when plugged into 4, yields: 240

$$eP'(t) + C'(t) = e \cdot Growth(P) - Loss(C) \quad (6)$$

Equation 6 allows us to think of our system as an open system from the point
242 of view of thermodynamics. Here *Growth* is the only source of the system, and

Loss is the only sink (see figure 6). All the energy exchange due to predation
 244 stays inside the system, so predation can be considered a closed subsystem.

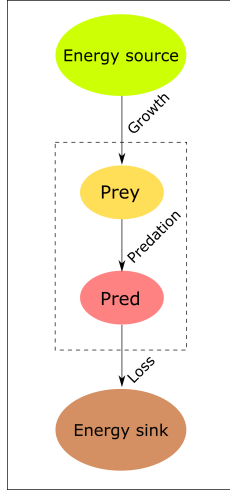


Figure 6: Plot showing the energy flow in our class of systems.

We can generalize this basic structure to multispecies, two trophic levels
 246 systems. First, we'll go back to equation 4 and just add more rows:

$$\begin{cases} P'_i(t) = Growth_i(P) - Predation_i(P_i, C) & : i = 1..n_P \\ C'_j(t) = -Loss_j(C_j) + GrossGrowth_j(P, C_j) & : j = 1..n_C \end{cases} \quad (7)$$

where now i runs from 1 to the number of prey n_P and j from 1 to the
 248 number of consumers n_C . Here, we've used P_i to denote the population of the
 prey labeled by i , and P for the vector containing all prey populations. Notice
 250 that while the *Growth* term can involve competition (and thus, depends on the
 whole vector P), the *Loss* term for species j depends only in the population of
 252 that species (i.e.: C_j), regardless of the rest.

Requiring once again our predation to be fully invested in consumer's growth,
 254 we find the following generalization of equation 5:

$$\sum_{j=1}^{n_C} \text{GrossGrowth}_j(P, C_j) = \sum_{i=1}^{n_P} e_i \cdot \text{Predation}_i(P_i, C) \quad (8)$$

Using 8 and 7, it is easy to prove that the multispecies generalization of 6

256 is:

$$\sum_{i=1}^{n_P} e_i P'_i(t) + \sum_{j=1}^{n_C} C'_j(t) = \sum_{i=1}^{n_P} e_i \cdot \text{Growth}_i(P) - \sum_{j=1}^{n_C} \text{Loss}_j(C_j) \quad (9)$$

The intuitive interpretation is, again, that the only sinks and sources of

258 energy in our systems are the total *Loss* and *Growth*.

Restriction 8 (or equivalently, 9) can be used to generalize realistic functional forms for the coupling terms. 260

A.1.2 Lotka-Volterra equations

The most basic model of predation is the Lotka-Volterra system of equations: 262

$$\begin{cases} P'(t) = rP - gPC \\ C'(t) = -lC + egCP \end{cases} \quad (10)$$

Where r represents the growth rate of the prey, g the grazing rate of the predator against the prey, l the loss rate of the predator and e the efficiency 264
conversion factor.

It is trivial to prove that the Lotka-Volterra model satisfies the requirements 266
shown in subsection A.1.1.

A.1.3 Multispecies Lotka-Volterra equations 268

Lotka-Volterra equations can be generalized to a model with multiple species by noting that each prey will be affected by all consumers, and each consumer 270
will be affected by all prey. In order to code the strength of this interactions, we introduce the matrix S , whose element S_{ji} gives the strength of the coupling 272
of consumer j and prey i . As a consequence, for prey dynamics this matrix is

scanned row-wise, while for predators it is scanned column-wise. The generalized system looks like: 274

$$\begin{cases} P'_i(t) = r_i P_i - P_i \sum_{j=1}^{n_C} g_j S_{ji} C_j & : i = 1..n_P \\ C'_j(t) = -l_j C_j + g_j e_j C_j \sum_{i=1}^{n_P} S_{ji} P_i & : j = 1..n_C \end{cases} \quad (11)$$

The fulfillment of condition 8 is again easily proven. 276

In this model, all terms can grow without boundaries. This is not only unrealistic, but also creates some problems from the sole point of view of mathematical stability. 278

280 **A.1.4 Rosenzweig-MacArthur model**

The Rosenzweig-MacArthur predator-prey model improves the previous model by adding boundaries to the terms' dependency on the prey population. This is achieved by encapsulating P inside saturating functions. In particular, the growth rate and the grazing rate r now depend on P (see equation 12 and compare it with 10). 284

$$\begin{cases} P'(t) = r(P)P - g(P)PC \\ C'(t) = -lC + eg(P)CP \end{cases} \quad (12)$$

Once again, condition 5 is trivially fulfilled independently of the functional form of $r(P)$ and $g(P)$. If both functions are chosen appropriately, we avoid unbounded growths. Typically, $r(P)$ and $g(P)$ are chosen so they generate a logistic growth and a Holling type II saturation response when plugged into 12. In mathematical terms, this means choosing $r(P) = r_0 \left(1 - \frac{P}{K}\right)$ and $g(P) = \frac{g_0}{P+H}$ (for more information see, for instance, [18]). After making this choices, our system takes its classical form: 290

292

$$\begin{cases} P'(t) = rP \left(1 - \frac{P}{K}\right) - gC \frac{P}{P+H} \\ C'(t) = -lC + egC \frac{P}{P+H} \end{cases} \quad (13)$$

A.1.5 Multispecies Rosenzweig-MacArthur model

Noticing the similarities between equations 10 and 12, the latter can be generalized in the same fashion as we did to obtain 11, yielding: 294

$$\begin{cases} P'_i(t) = r_i(P)P_i - P_i \sum_{j=1}^{n_C} g_j(P)S_{ji}C_j & : i = 1..n_P \\ C'_j(t) = -l_jC_j + g_j(P)e_jC_j \sum_{i=1}^{n_P} S_{ji}P_i & : j = 1..n_C \end{cases} \quad (14)$$

Written like this, it is easy to see that the condition 8 is fulfilled. 296

Regarding the proper functional forms of $r_i(P)$ and $g_j(P)$, our growth term has to take into account both the inter and intraspecific competition. This can be easily modelled by choosing: 298

$$r_i(P) = r_i \left(1 - \sum_{k=1}^{n_P} A_{ik}P_k\right) \quad (15)$$

where the matrix elements A_{ik} account for the intensity of the competition caused by species k on species i . Thus, non-diagonal elements account for interspecific competition, and diagonal ones for intraspecific competition. 300

We hypothesize that the grazing rates corresponding to predator j , that is, $g_j(P)$, follow a Holling type II functional response dependent on the total consumption of prey by predator j : 302

$$g_j(P) = \frac{g_j}{\sum_{i=1}^{n_P} S_{ji}P_i + H_j} \quad (16)$$

	Two species	Multispecies
Lotka-Volterra	$\begin{cases} P'(t) = rP - gPC \\ C'(t) = -lC + egCP \end{cases}$	$\begin{cases} P'_i(t) = r_i P_i - P_i \sum_{j=1}^{n_C} g_j S_{ji} C_j \\ C'_j(t) = -l_j C_j + g_j e_j C_j \sum_{i=1}^{n_P} S_{ji} P_i \end{cases}$
Rosenzweig-MacArthur	$\begin{cases} P'(t) = r(P)P - g(P)PC \\ C'(t) = -lC + eg(P)CP \end{cases}$	$\begin{cases} P'_i(t) = r_i(P) P_i - P_i \sum_{j=1}^{n_C} g_j(P) S_{ji} C_j \\ C'_j(t) = -l_j C_j + g_j(P) e_j C_j \sum_{i=1}^{n_P} S_{ji} P_i \end{cases}$

Table 2: Summary table with the different types of predation models studied. Written this way, the parallelisms are obvious. In multispecies models, the index i runs from 1 to n_P , and j from 1 to n_C . The functional forms of $r_i(P)$ and $g_j(P)$ are given in equations 15 and 16. In the present paper we used the Rosenzweig-MacArthur multispecies model, that is, the one in the lower right corner.

A.2 Chaos detection

In the exploratory phase of this research three parallel approaches to chaos detection were followed: Lyapunov exponents estimation [22], Gottwald - Melbourne θ -1 test [20] and visual inspection. Despite differences in the exact probabilities, the three of them led us to the same qualitative conclusions (see figure 7). We found the Gottwald - Melbourne test to be the fastest and most reliable of all.

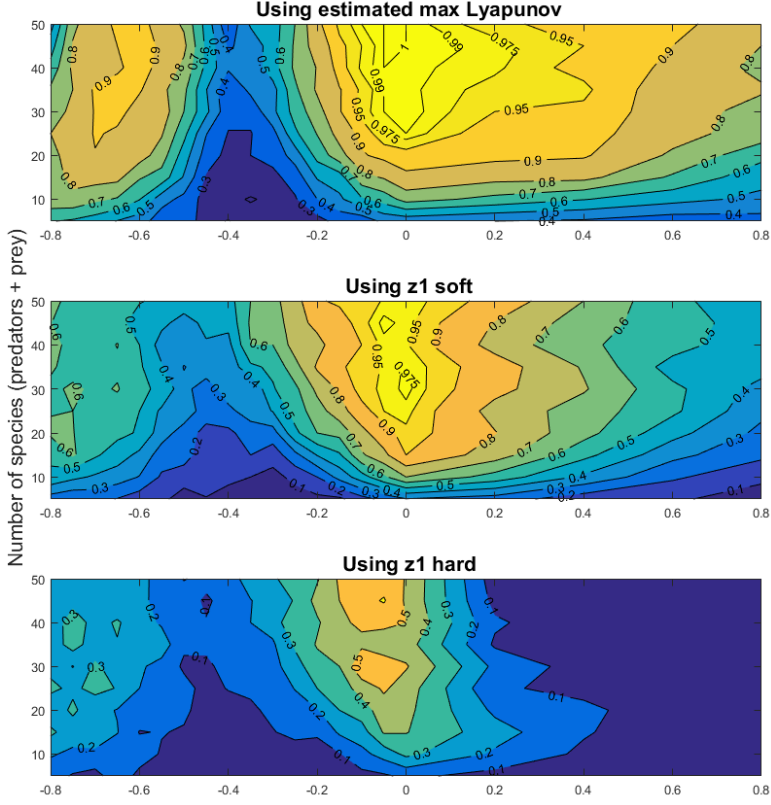


Figure 7: Performing the same analysis with different chaos detection algorithms we found different numerical results. The upper panel used the estimation of the maximum Lyapunov exponent as a test for chaoticity. The second and third used the $z1$ Gottwald - Melbourne test, with different degrees of tolerance. In particular, $z1$ *soft* is more prone to classify complicated cycles as chaos, and $z1$ *hard* is more likely to throw indecisive results. Even for the most conservative test ($z1$ *hard*), the qualitative conclusions (that is, that chaos happens more frequently in the vicinity of neutral competition) still hold.

314 A.2.1 Melbourne-Gottwald 0-1 test in a nutshell

The 0-1 test for chaos is designed for distinguishing between regular and chaotic
 316 dynamics in deterministic systems. It works directly with the observed time
 series, so a prior knowledge of the underlying dynamics is not required (as long
 318 as we know that they are deterministic).

This short section is more a motivation than a rigorous proof. A minimal,
 intuitive approach to the method will be outlined. For a detailed, complete
 320 explanation please refer to [20].

First, we have to use one of our time series of observations ϕ_k to build the
 322 functions:

$$\begin{cases} p_n(\theta) = \sum_{k=1}^n \phi_k \cos(k\theta) \\ q_n(\theta) = \sum_{k=1}^n \phi_k \sin(k\theta) \end{cases} \quad (17)$$

Using Euler's formula both equations can be given a more compact form: 324

$$z_n(\theta) = p_n(\theta) + iq_n(\theta) = \sum_{k=1}^n \phi_k e^{ik\theta} \quad (18)$$

In the complex plane, $e^{ik\theta}$ represents a unit vector pointing in the direction
 $k\theta$. So each observation in our time series can be understood as the size of a
 326 step, being $k\theta$ its direction (see table 3).



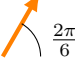
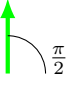




k	0	1	2	3	...
$k\theta$	0	$\frac{\pi}{6}$	$\frac{2\pi}{6}$	$\frac{\pi}{2}$...
$e^{ik\theta}$					...
ϕ_k	2	1	0.5	0.25	...
$\phi_k e^{ik\theta}$					...

Table 3: Example showing a step by step geometrical construction of the elements inside the summation operator in equation 18. In this example we use a time series whose first elements are $\phi_j = \{2, 1, 0.5, 0.25, \dots\}$. The parameter θ has been set to $\frac{\pi}{6}$.

Adding up the elements in table 3 as indicated by equation 18 can be interpreted geometrically as vector addition, i.e., performing one "step" after another (see figure 8).

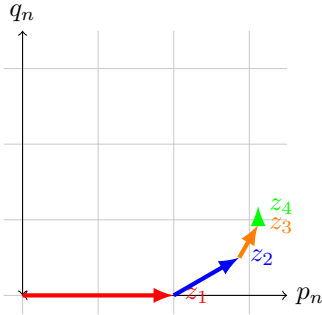


Figure 8: Geometrical calculation of z_1, z_2, z_3 and z_4 for $\phi_j = \{2, 1, 0.5, 0.25, \dots\}$ and $\theta = \frac{\pi}{6}$.

With this picture in mind, it is easy to understand the kind of paths that different types of time series will give rise to (see figure 9). Constant time series generate cyclic paths (polygons) or pseudocyclic paths (polygons that do not close after a first round). Periodic or pseudoperiodic time series generate periodic or pseudoperiodic paths (note that the summand in 18 becomes then

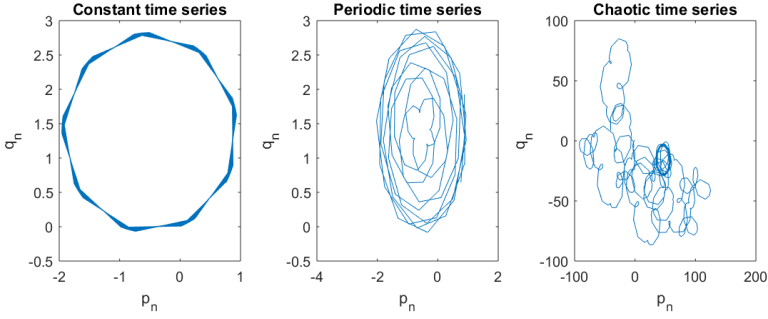


Figure 9: First and second panels show the paths generated by the $z1$ test when applied to constant and periodic time series. The third panel shows the case with a chaotic time series (notice the different scale). While in the first two cases the paths remain inside a bounded domain, in the chaotic case the path drifts away from the starting point in a brownian-motion-like fashion.

the product of two periodic/pseudoperiodic functions). Random time series generate brownian-motion-like paths. Provided that our system is deterministic, the apparent stochasticity of our observed time series is a strong indicator of chaos.

The case of an underlying chaotic time series is the only one that generates a path that doesn't stay inside a bounded domain around the starting point. The $z1$ test uses the mean square displacement as a measure of this drift. The system is considered to be chaotic if the square displacement keeps growing for large times. If, on the contrary, it stays bounded, the test will consider the system not chaotic.

A.3 Neutral competition and system dimensionality

If we drop everything but the competition part of our dynamics (see equation 14), we will find a system of n_P equations like the following:

$$P'_i(t) = rP_i \left(1 - \frac{1}{K} \sum_{k=1}^{n_P} A_{ik} \cdot P_k \right) : i = 1..n_P \quad (19)$$

In order to model a neutral competition, we should use the same competition coefficient for each interaction between species. That is, take $A_{ik} = A$ for all i and k . Equation 19 then becomes:

$$P'_i(t) = rP_i \left(1 - \frac{A}{K} \sum_{k=1}^{n_P} P_k \right) \quad : i = 1..n_P \quad (20)$$

From equation 20 we see that all species have exactly the same dynamical equation. This will make the nullclines to coincide at all points, so the equilibrium points will degenerate to equilibrium hyperplanes (see figure 10).

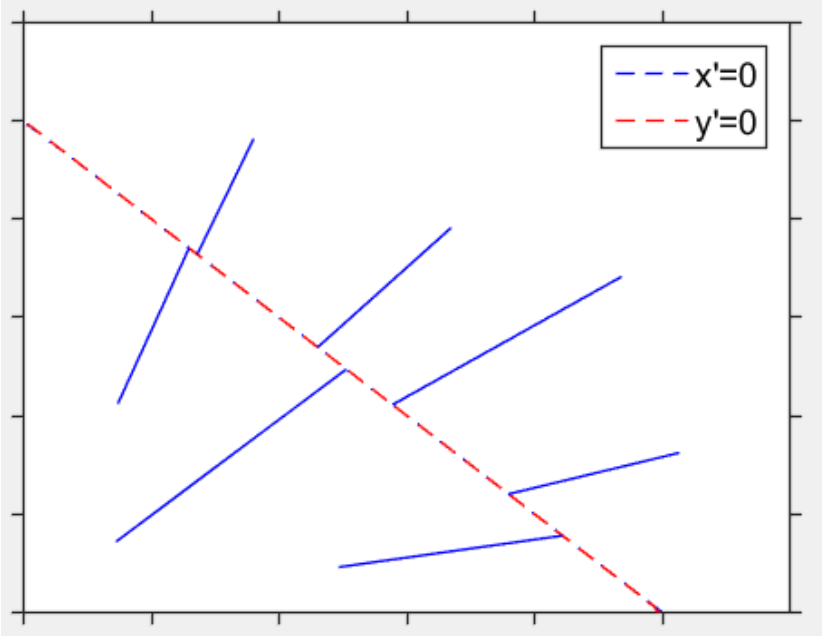


Figure 10: Example with 2 prey under neutral competition. Both nullclines coincide point to point, giving rise to a higher dimensional equilibrium hyperplane (in this case, a straight line)

This problem can be solved noticing that, in a competition-only system, the effect of neutrality is to fade out the differences between species. If this is the case, the labels i distinguishing them become meaningless. It is a natural idea to sum up all the biomasses of competing species into a new variable, that of

total population of (now indistinguishable) species, defined by:

$$T(t) = \sum_{i=1}^{n_P} P_i(t) \quad (21)$$

In agreement with the biological intuition, manipulating 21 and 20 it can 360
be proved (see eq. 22), that the total population biomass will follow the same
differential equation as the individual species abundances (i.e., equation 20). 362

$$T'(t) = \sum_{i=1}^{n_P} P'_i(t) = r \sum_{i=1}^{n_P} P_i \left(1 - \frac{A}{K} \sum_{k=1}^{n_P} P_k \right) = rT \left(1 - \frac{A}{K} T \right) \quad (22)$$

Additionally, this result shows that we are actually working with a one-
dimensional system. The apparent n_P dimensions of our original problem were 364
an artifact due to a wrong choice of state variables. In our model, the predation
interaction breaks this excess of symmetry, so we can still work with neutral 366
competition as long as the predation is not neutral without facing problems of
decay in system dimensionality. 368

A.4 Extra figures

A.4.1 Multispecies predator-prey network

370

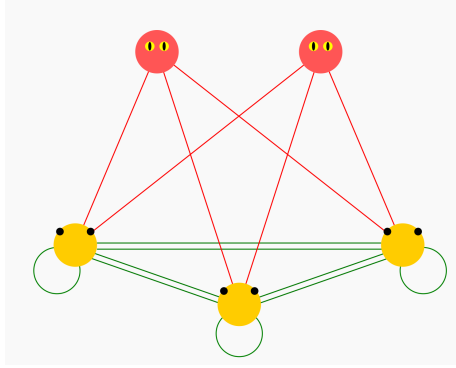


Figure 11: Example with 2 consumers and 3 prey. Each one of the red links represents a predation interaction (coded in the matrix of predator preference coefficients, S). Each green link represents a competition interaction (coded in the matrix of competition coefficients, A). The closed green loops are related with carrying capacity (diagonal elements of A) interpreted here as intra-species competition.

A.4.2 Probabilities grouped by number of species

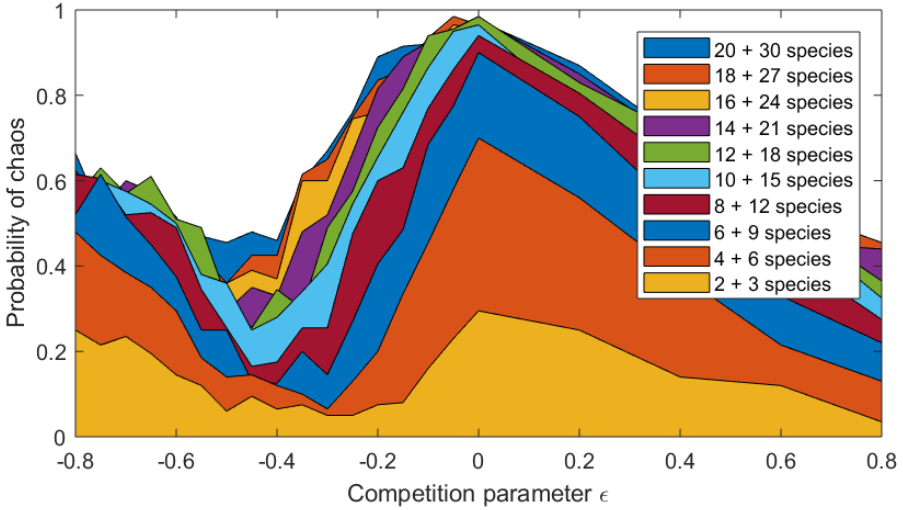


Figure 12: Summary of the results of the whole set of simulations. The competition parameter ϵ is on the horizontal axis. The estimated probability of chaos is represented on the vertical one. Each panel corresponds to an ecosystem with a different number of interacting species. The exact number is shown in each box, as number of predators + number of prey.

A.4.3 Flow chart

372

In the spirit of reproducible research we made available all the analysis code used to draw our conclusions. Any interested researcher can clone it from a *GitHub* repository [21] and, executing a single script, reproduce all our simulations and figures. This figure shows schematically what this script does:

374

376

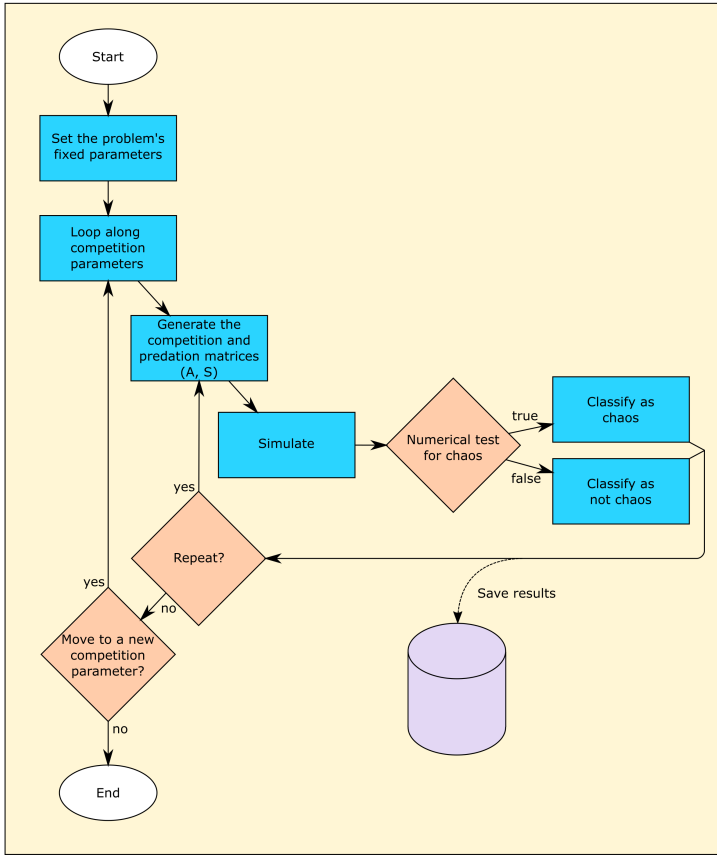


Figure 13: Flow chart describing the numerical experiment. The source code is available at <https://doi.org/10.5281/zenodo.1319590>.

References

- [1] Macarthur R, Levins R. The Limiting Similarity, Convergence, and Divergence of Coexisting Species. *The American Naturalist*. 1967;101(921):377–385. Available from: <https://doi.org/10.1086/282505>. 378 380
- [2] Hutchinson GE. Homage to Santa Rosalia or Why Are There So Many Kinds of Animals? *The American Naturalist*. 1959 may;93(870):145–159. Available from: <https://doi.org/10.1086/282070>. 382
- [3] Hutchinson GE. The Paradox of the Plankton. *The American Naturalist*. 1961 may;95(882):137–145. Available from: <https://doi.org/10.1086/282171>. 384 386
- [4] Winter C, Bouvier T, Weinbauer MG, Thingstad TF. Trade-Offs between Competition and Defense Specialists among Unicellular Planktonic Organisms: the "Killing the Winner" Hypothesis Revisited. *Microbiology and Molecular Biology Reviews*. 2010 mar;74(1):42–57. Available from: <https://doi.org/10.1128/MMBR.00034-09>. 388 390
- [5] Hubbell SP. The Unified Neutral Theory of Biodiversity and Biogeography. *Biological Conservation*. 2003 apr;110(2):305. Available from: [https://doi.org/10.1016/S0006-3207\(02\)00228-8](https://doi.org/10.1016/S0006-3207(02)00228-8). 392 394
- [6] Scheffer M, van Nes EH. Self-organized similarity, the evolutionary emergence of groups of similar species. *Proceedings of the National Academy of Sciences*. 2006 apr;103(16):6230–6235. Available from: <https://doi.org/10.1073/pnas.0508024103>. 396 398
- [7] Scheffer M, van Nes EH, Vergnon R. Toward a unifying theory of biodiversity. *Proceedings of the National Academy of Sciences*. 2018 jan;115(4):201721114. Available from: <https://doi.org/10.1073/pnas.1721114115>. 400 402

[8] Fort H, Scheffer M, van Nes EH. The paradox of the clumps mathematically explained. *Theoretical Ecology*. 2009 sep;2(3):171–176. Available from: <https://doi.org/10.1007/s12080-009-0040-x>.

[9] Fort H, Scheffer M, Van Nes E. The clumping transition in niche competition: A robust critical phenomenon. *Journal of Statistical Mechanics: Theory and Experiment*. 2010 may;2010(5):P05005. Available from: <https://doi.org/10.1088/1742-5468/2010/05/P05005>.

[10] Vergnon R, Leijds R, van Nes EH, Scheffer M. Repeated Parallel Evolution Reveals Limiting Similarity in Subterranean Diving Beetles. *The American Naturalist*. 2013 jul;182(1):67–75. Available from: <https://doi.org/10.1086/670589>.

[11] Scheffer M, Vergnon R, van Nes EH, Cuppen JGM, Peeters ETHM, Leijds R, et al. The Evolution of Functionally Redundant Species; Evidence from Beetles. *PLOS ONE*. 2015 oct;10(10):e0137974. Available from: <https://doi.org/10.1371/journal.pone.0137974>.

[12] Segura AM, Kruk C, Calliari D, García-Rodríguez F, Conde D, Widdicombe CE, et al. Competition drives clumpy species coexistence in estuarine phytoplankton. *Scientific Reports*. 2013 dec;3(1):1037. Available from: <https://doi.org/10.1038/srep01037>.

[13] Vergnon R, van Nes EH, Scheffer M. Emergent neutrality leads to multimodal species abundance distributions. *Nature Communications*. 2012;3(May 2011):663. Available from: <https://doi.org/10.1038/ncomms1663>.

[14] Huisman J, Weissing FJ. Biodiversity of plankton by species oscillations and chaos. *Nature*. 1999 nov;402(6760):407–410. Available from: <https://doi.org/10.1038/46540>.

- [15] Benincà E, Huisman J, Heerkloss R, Jöhnk KD, Branco P, Van Nes EH, et al. Chaos in a long-term experiment with a plankton community. *Nature*. 2008 feb;451(7180):822–825. Available from: <https://doi.org/10.1038/nature06512>. 430
- [16] Rosenzweig ML, MacArthur RH. Graphical Representation and Stability Conditions of Predator-Prey Interactions. *The American Naturalist*. 1963 jul;97(895):209–223. Available from: <https://doi.org/10.1086/282272>. 434
- [17] van Nes EH, Scheffer M. Large Species Shifts Triggered by Small Forces. *The American Naturalist*. 2004 aug;164(2):255–266. Available from: <https://doi.org/10.1086/422204>. 436
- [18] Edelstein-Keshet L. *Mathematical Models in Biology*. Society for Industrial and Applied Mathematics; 2005. Available from: <https://doi.org/10.1137/1.9780898719147>. 438
- [19] Dakos V, Beninca E, van Nes EH, Philippart CJM, Scheffer M, Huisman J. Interannual variability in species composition explained as seasonally entrained chaos. *Proceedings of the Royal Society B: Biological Sciences*. 2009 aug;276(1669):2871–2880. Available from: <https://doi.org/10.1098/rspb.2009.0584>. 440
- [20] Gottwald GA, Melbourne I. On the Implementation of the 0-1 Test for Chaos. *SIAM Journal on Applied Dynamical Systems*. 2009 jan;8(1):129–145. Available from: <https://doi.org/10.1137/080718851>. 442
- [21] Rodríguez-Sánchez P. PabRod/Chaos-and-neutrality: Analysis script for "Neutral competition boosts chaos in food webs"; 2018. Available from: <https://doi.org/10.5281/zenodo.1319590>. 444
- [22] Strogatz SH. *Nonlinear Dynamics And Chaos: With Applications To Physics, Biology, Chemistry And Engineering*; 1994. 446

- [23] Thebault E, Fontaine C. Stability of Ecological Communities and the Architecture of Mutualistic and Trophic Networks. *Science*. 2010 aug;329(5993):853–856. Available from: <https://doi.org/10.1126/science.1188321>. 456 458
- [24] Huisman J, Johansson AM, Folmer EO, Weissing FJ. Towards a solution of the plankton paradox: the importance of physiology and life history. *Ecology Letters*. 2001 sep;4(5):408–411. Available from: <https://doi.org/10.1046/j.1461-0248.2001.00256.x>. 460 462
- [25] Schippers P, Verschoor AM, Vos M, Mooij WM. Does "supersaturated coexistence" resolve the "paradox of the plankton"? *Ecology Letters*. 2001 sep;4(5):404–407. Available from: <https://doi.org/10.1046/j.1461-0248.2001.00239.x>. 464 466